CHARACTERISTICS ANALYSIS OF REPETITION FREQUENCY HIGH-POWER MICROWAVE PULSES IN ATMOSPHERE

T. Tang, C. Liao, and W. B. Lin

Institute of Electromagnetics
Southwest Jiaotong University, Chengdu 610031, China

Abstract—A semi-analytical model for the propagation of the repetition frequency high power microwave (HPM) pulses is established. The effects of different parameters of the repetition frequency HPM pulses on air breakdown are analyzed. A critical repetition frequency for the HPM pulse is presented under which the electron density does not exceed that of the air breakdown when the individual pulse arrives. The prediction for the critical repetition frequency and the threshold of the air breakdown due to the repetition frequency HPM pulses is demonstrated with several numerical simulations.

1. INTRODUCTION

With the development of the source technology [1–3], in particular, the development of high repetition frequency and miniaturization technology, the repetition frequency HPM pulses have important applications in many fields, such as electronic countermeasures and communications interference [4–6].

There are two kinds of the repetition frequency HPM sources: narrowband and ultra-wideband (UWB). The narrowband source generally concentrates in the X-band, its equivalent radiated power (ERP) has the order of magnitude greater than GW, pulse width is about tens ns, and the repetition frequency is about several hundred Hz. The UWB one is generally in L-band, its ERP also larger than GW, the output pulse width ranges from a few nanoseconds to tens of nanoseconds, and the repetition frequency is close to KHz [7]. The propagation of the repetition frequency

HPM pulses in atmosphere will cause non-linear physical processes, and this phenomenon has received attention in recent years. For example, Ref. [8] investigated the relationship between the number of the penetrated pulses and the microwave power under different atmospheric pressure and microwave pulse parameters, and Ref. [9] analyzed the attachment and recombination effects in the electronic relaxation process.

When the air breakdown happens, the electron density in the atmosphere will increase dramatically in a short time [10, 11], we call this duration as the ionization time. However, within the interval time (also called the "relaxation time") between two pulses, electrons will combine with the neutral molecule (such as e+O_2 and e+$2O_2$ [12]), those processes will lead to decreasing the electron density. Therefore, before the arrival of the next pulse, the initial electron density of the atmosphere has been changed, and this will affect the propagation of the follow-up pulses.

In this work, a semi-analytical model for the propagation of the repetition frequency HPM pulses is presented. Starting with the continuity equation, which describes the electron density evolution due to the repetition frequency HPM pulses, we analyze the effects of different parameters of the repetition frequency HPM pulses on the air breakdown threshold, such as single pulse field intensity, pulse width and repetition frequency etc. In particular, a critical repetition frequency under which the pulses reaches the electron density is equal to that of the air breakdown is investigated. The air breakdown criterion for the propagation of the repetition frequency HPM pulses propagates in the atmosphere has been derived. The numerical results provide insights for the air breakdown process due to the repetition frequency HPM pulses.

2. SEMI-ANALYTICAL MODEL

The evolution of electron density in air due to the HPM pulses can be described by the continuity equation,

$$\frac{\partial N_e}{\partial t} = (v_i - v_l) N_e, \tag{1}$$

where N_e is the electron density in m^{-3}, v_i and v_l denote the ionization frequency and the loss frequency, respectively, the loss has three mechanisms: electron-ion recombination, electron-molecule attachment and diffusion [13]. But compared to the contribution of the attachment, the effects of the other two can be ignored [9, 14]. So the solution of Equation (1) can be written as $N_e(t) = N_{e0} \exp(v_i t - v_a t)$ where v_a denotes the attachment frequency.

Before the pulse leaves, the loss terms is negligible, and the ionization dominates. Within the relaxation time, the attachment losses will dominate, and this leads electron density decreases quickly. Therefore, when the repetition frequency HPM pulse propagates through the atmosphere, the electron density will changes according to the following rules:

During the ionization time due to the first pulse, the evolution of the electron density can be approximated as

$$N_{e1} \simeq N_{e0} \exp(v_i \tau), \tag{2}$$

where τ is the pulse width of each single pulse and N_{e0} can be estimated using the following formula [15], where h is the altitude in km,

$$N_{e0} \simeq \begin{cases} 10 & (h < 25\,\text{km}) \\ 8 \times 10^7 \times (h/60)^{18} & (h \geq 25\,\text{km}) \end{cases}, \tag{3}$$

During the first relaxation time, the electron density can be approximated as

$$N_{e11} \simeq N_{e1} \exp(-v_a t_{r1}) \simeq N_{e0} \exp(v_i \tau - v_a t_{r1}), \tag{4}$$

where the attachment frequency v_a can be approximated as [16]

$$v_a \simeq 10^5 p, \tag{5}$$

And p is the atmosphere pressure in Torr, t_{r1} is the relaxation time between the first pulse and the second pulse. For convenience, we use t_r to represent the following relaxation time.

During the second ionization time, the electron density can be written as follows

$$N_{e2} \simeq N_{e11} \exp(v_i \tau) \simeq N_{e0} \exp(v_i 2\tau - v_a t_r), \tag{6}$$

During the second relaxation time, the electron density evolutes as

$$N_{e22} \simeq N_{e2} \exp(-v_a t_r) \simeq N_{e0} \exp(v_i 2\tau - v_a 2 t_r), \tag{7}$$

. . .

During the $(N-1)$th ionization time,

$$N_{e(N-1)} = N_{e(N-2)(N-2)} \exp(v_i \tau) = N_{e0} \exp\left(v_i(N-1)\tau - v_a(N-2)t_r\right), \tag{8}$$

During the $(N-1)$th relaxation time,

$$\begin{aligned} N_{e(N-1)(N-1)} &= N_{e(N-1)} \exp(-v_a t_r) \\ &= N_{e0} \exp\left(v_i(N-1)\tau - v_a(N-1)t_r\right), \end{aligned} \tag{9}$$

Note that $v_i \gg v_a$.

Usually $N_p = 10^8 N_{e0}$ is taken as the critical electron density for the air breakdown condition [17, 18]. So, we define a critical frequency

f_c for the N repetition frequency HPM pulses, under which the electron density in the air will not exceed N_p after every relaxation time between two pulses. If the repetition frequency of the HPM pulses is lower than this critical frequency, we can think the previous pulses will have very small effects on the propagation of the subsequent pulses. Since $N_{e11} < N_{e22} \ldots < N_{e(N-1)(N-1)}$, so the critical repetition frequency f_c can be obtained

$$f_c \leq \frac{v_a}{v_i\tau - \ln(10^8)/(N-1)}. \tag{10}$$

When the electron density reaches the critical density N_p, from Equation (8), we have

$$v_i = \frac{\ln(10^8) + v_a(N-2)t_r}{(N-1)\tau}, \tag{11}$$

Since the ionization frequency v_i is a function of electric field strength, the threshold of the air breakdown can be obtained from Equation (11).

3. NUMERICAL EXAMPLES

3.1. Propagation in Lower Atmosphere

When the repetition frequency HPM pulses propagate in the lower atmosphere, the ionization frequency can be expressed as

$$v_i = \alpha\mu E_e, \tag{12}$$

where $\alpha \simeq 10^{-4}\left(E_e/p - 26\right)^2 p$ denotes Townsend's first ionization coefficient [17], $\mu = e/\left(mv_c\right)$ is the electron mobility in the effective field, E_e in V/cm, which is related to the rms wave field strength by the relation $E_e^2 = E_{rms}^2/\left(1 + \omega^2/v_c^2\right)$, ω is the angular frequency of each individual pulse, and $v_c \simeq 5 \times 10^9 p$ is the electron collision frequency [12, 18]. In the lower atmosphere, we have $\omega \ll v_c$, which implies that $E_e \simeq E_{rms}$. So in the considered altitude range, Equation (12) can be applied to both the narrow-band and the UWB ones.

Substituting Equations (12) and (5) into (10), we have

$$f_c \leq \frac{1 \times 10^5 p}{3.5 \times 10^{-3}(E_e/p - 26)^2 E_e\tau - 18.4/(N-1)}, \tag{13}$$

Combining Equations (11) and (12), we can get

$$(E_e/p - 26)^2 E_e = \frac{18.4 + 1 \times 10^5 p\,(N-2)\,t_r}{3.5 \times 10^{-3}\,(N-1)\,\tau}, \tag{14}$$

After taking cube root of this Equation (14), we obtain the air breakdown threshold E_b in the lower atmosphere

$$E_b = 2.9 \times 10^{-4} \frac{\beta^{1/3}}{a} + 2.56 \times 10^7 \frac{p^2 a}{\beta^{1/3}} + 17.3p, \qquad (15)$$

where

$$\beta = p^2 a^2 \left\{ -2.57 \times 10^{19} pa + 5.63 \times 10^{18} b + 1.04 \times 10^{20} \right.$$

$$\left. + \left[1.58 \times 10^{25} apb + 1.72 \times 10^{24} b^2 + 6.34 \times 10^{25} b - 2.92 \times 10^{26} \right]^{1/2} \right\}, (16)$$

And

$$a = (N - 1)\,\tau, \ \ b = v_a (N - 2)\,t_r. \qquad (17)$$

Note that $p = 760 \exp(-h/7)$.
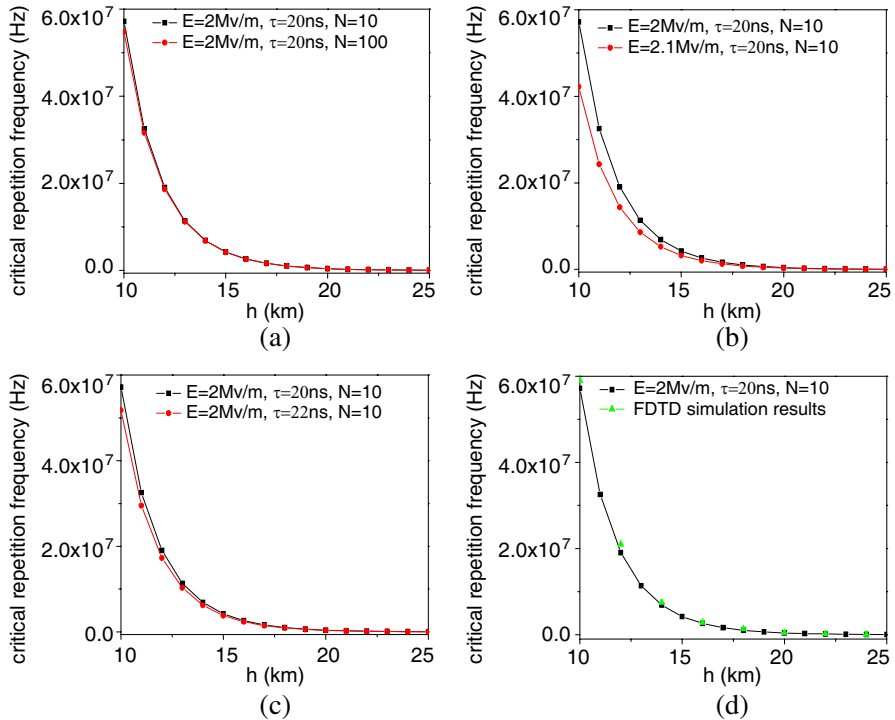
Figure 1. The relation between the critical repetition frequency and the altitude in the lower atmosphere. (a) different pulse number N; (b) different electrical field intensity E_e; (c) different single-pulse width τ; (d) the comparison between the FDTD simulation and the semi-analytical calculation.

From Equation (13), one can see that the repetition frequency will decrease as the increasing of the field intensity E_e, the single-pulse width τ and the total pulse number N. The critical repetition frequency f_c vs. altitude are shown in Fig. 1. In Fig. 1, we can see that the changes in the electric field intensity E_e have a large impact on the critical repetition frequency, and the changes in pulse number N have little effects. Fig. 2 shows the relation between E_b and altitude h. It can be seen that the breakdown threshold E_b is about $1.48\,\mathrm{Mv/m}$ at altitude of $10\,\mathrm{km}$ for $N = 10$, $\tau = 20\,\mathrm{ns}$, $t_r = 50\,\mathrm{ns}$.

In order to validate the semi-analytical model, we employ the finite-difference time-domain (FDTD) method to compute the critical frequency and the air breakdown. The HPM atmospheric propagation
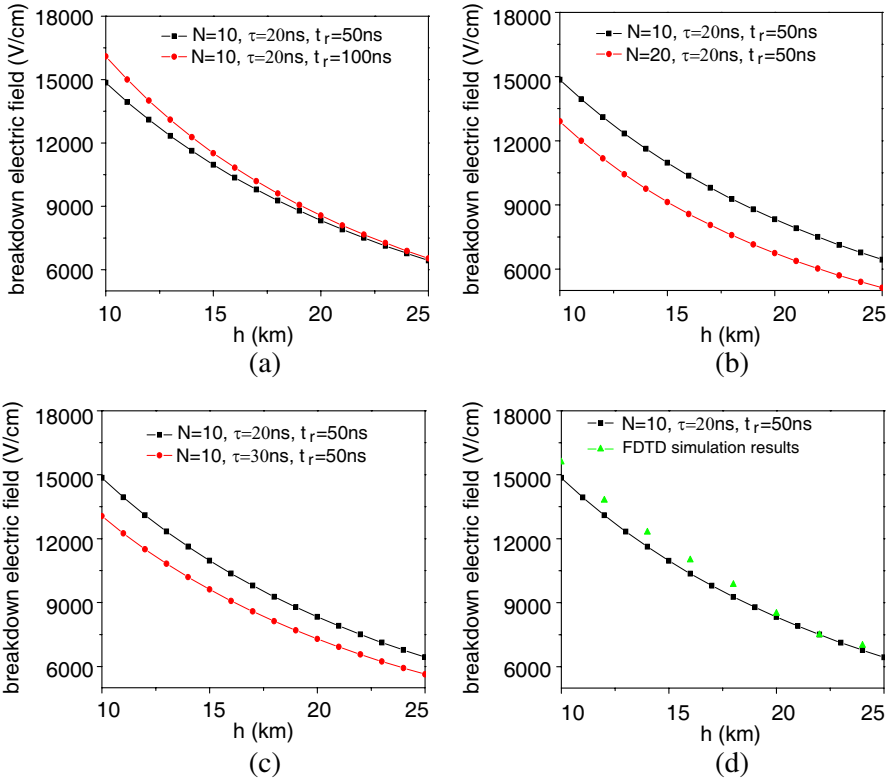
Figure 2. The relation between the breakdown threshold and the altitude in the lower atmosphere. (a) different relaxation time t_r; (b) different pulse number N; (c) different single-pulse width τ; (d) the comparison between the FDTD simulation and the semi-analytical calculation.

is governed by Maxwell equations and the electronics magneto hydrodynamic equations [12, 13]:

$$\nabla \times \mathbf{E} = -\frac{\partial \mathbf{B}}{\partial t}, \tag{18}$$

$$\nabla \times \mathbf{H} = \mathbf{J} + \frac{\partial \mathbf{D}}{\partial t}, \tag{19}$$

$$\frac{\partial n}{\partial t} = (v_i - v_a) n - \nabla_z \cdot (n\mathbf{u}), \tag{20}$$

$$m\frac{\partial (n\mathbf{u})}{\partial t} = en (\mathbf{E} + \mathbf{u} \times \mathbf{B}) - nmv_c\mathbf{u} - \nabla_z \cdot (n\varepsilon_e), \tag{21}$$

$$\frac{\partial (n\varepsilon_e)}{\partial t} = en (\mathbf{u} \cdot \mathbf{E}) - nv_i\varepsilon_e - nv_\omega\varepsilon_e, \tag{22}$$

Which can be numerically solved by the FDTD method given in [19]. The comparisons of the simulation results between these two methods are shown in Fig. 1(d) and Fig. 2(d), respectively. It can be seen that these two solutions agree with each other very well. Due to space limitation, here we only show the case for $E_e = 2\,\mathrm{Mv/m}$, $\tau = 20\,\mathrm{ns}$ and $N = 10$ in Fig. 1(d), and $N = 10$, $\tau = 20\,\mathrm{ns}$ and $t_r = 50\,\mathrm{ns}$ in Fig. 2(d). For the other different parameters, the agreements between these two methods are similar. Note that the computational cost of FDTD is much higher than those of the semi-analytical model.

3.2. Propagation in High-altitude Atmosphere

For the altitude higher than $25\,\mathrm{km}$, ω is close to v_c, In this case, we need to consider the narrow-band pulses and the UWB ones separately.

For the narrow-band pulses, the ionization frequency can be approximated as [12]

$$v_i \simeq 5.14 \times 10^{11} p \exp\left(-73\alpha^{-0.44}\right), \tag{23}$$

where $\alpha = E_e/[p^2 + (1.26f_{\mathrm{GHz}})^2]^{1/2}$, f_{GHz} is the carrier frequency in GHz.

Substituting Equations (23) and (5) into (10), we have

$$f_c \leq \frac{1 \times 10^5 p}{5.14 \times 10^{11} \exp\left[-73 \Big/ \left(E_e/\left(p^2 + 1.588f_{\mathrm{GHz}}^2\right)^{1/2}\right)^{0.44}\right] p\tau - 18.4/(N-1)}. \tag{24}$$

Combining Equations (11) and (23), we obtain the breakdown threshold E_b

$$E_b = \left[p^2 + (1.26f_{\mathrm{GHz}})^2\right]^{1/2} \left(73 \Big/ \ln\left[\frac{5.14 \times 10^{11} p(N-1)\tau}{18.4 + 10^5 p(N-2)t_r}\right]\right)^{2.27}. \tag{25}$$

Figures 3(a)–(c) and 4(a)–(c) show the critical repetition frequency and the breakdown threshold for a narrowband repetition frequency HPM pulse whose carrier frequency is 10 GHz.

From Fig. 3, we can see that there is a minimum for the critical repetition frequency at some altitude. It first decreases with altitude and reaches a minimum, then it increases with the altitude. This is consistent with the breakdown curves shown in Fig. 4.

The comparisons of the solutions between these two methods are given in Fig. 3(d) and Fig. 4(d). It can be seen that these two solutions agree with each other very well.

For the case of UWB, the effective electric field E_e for an arbitrary
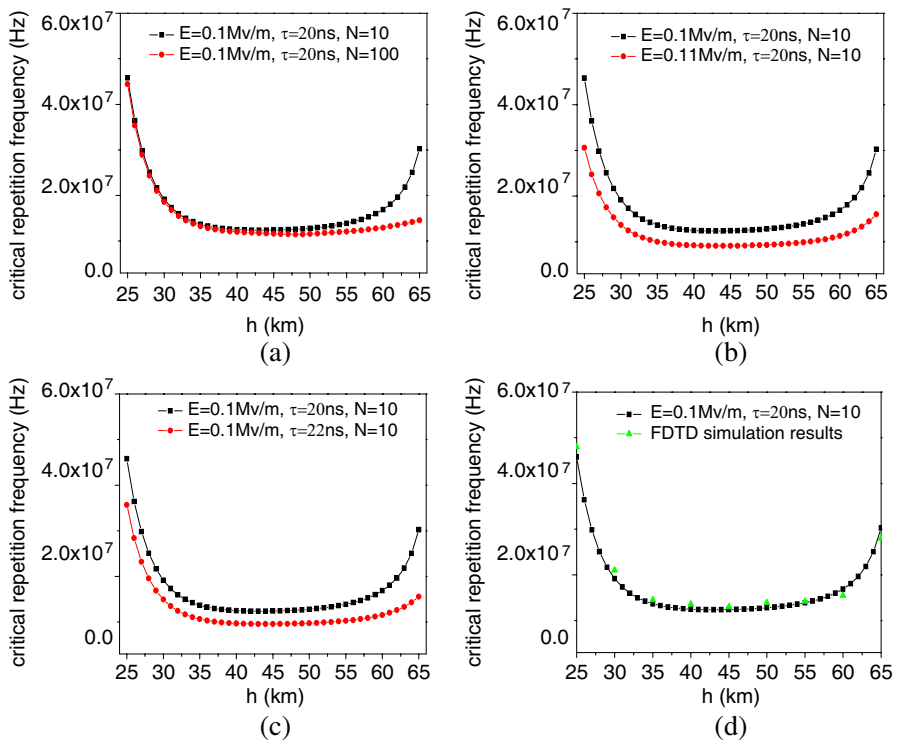
Figure 3. The relation between the critical repetition frequency and the altitude in high-altitude atmosphere for a narrowband case. (a) different pulse number N; (b) different electrical field intensity E_e; (c) different single-pulse width τ; (d) the comparison between the FDTD simulation and the semi-analytical calculation.
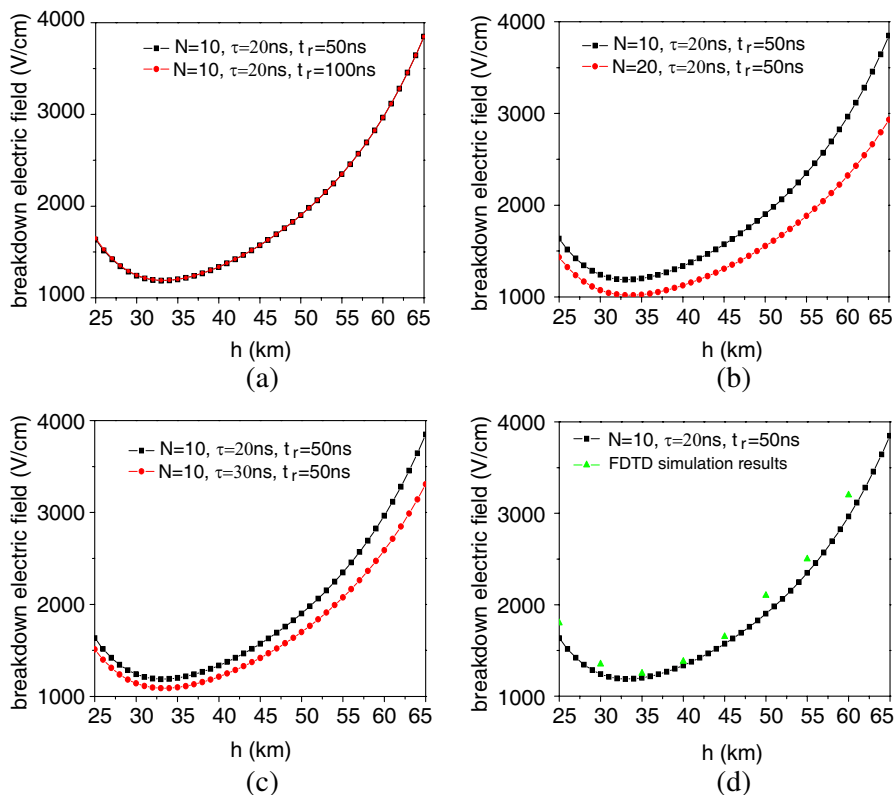
Figure 4. The relation between the breakdown threshold and the altitude in high-altitude atmosphere for a narrowband case. (a) different relaxation time t_r; (b) different pulse number N; (c) different single-pulse width τ; (d) the comparison between the FDTD simulation and the semi-analytical calculation.

electromagnetic pulse can be written as [20]

$$E_e = \sqrt{1/2}mq^{-1}\sqrt{\langle u(\tau)^2 \rangle}v_c, \tag{26}$$

where q and m denote the electron charge and mass, respectively; $u(\tau)$ is the electron fluid velocity in the atmosphere, and $\langle u(\tau)^2 \rangle$ is the mean square of electron velocity which can be calculated by [20]

$$\langle u(\tau)^2 \rangle = \frac{1}{\tau} \int_0^\tau u(t)u(t)^* dt, \tag{27}$$

where $u(t)^*$ indicates the complex conjugate of the velocity.

The collision frequency v_c and the ionization frequency v_i were fitted from the experimental data, which are related to the pressure and the effective field as follows [21]

$$v_c/p = \begin{cases} 3.24 \times 10^8 (E_e/p)/\left[1 + 0.04(E_e/p)\right] & 30 \leq E_e/p \leq 54 \\ 2.93 \times 10^8 (E_e/p) \times \left[1 + 0.041(E_e/p)\right] & 54 < E_e/p \leq 120 \\ 5.2 \times 10^8 \times (E_e/p)^{1/2} & 120 < E_e/p \leq 3000 \end{cases} , (28)$$

$$v_i/p = \begin{cases} \left[1.32 + 0.054(E_e/p)\right] \times 10^7 \exp(-208p/E_e) & 30 \leq E_e/p \leq 54 \\ \left[5.0 + 0.19(E_e/p)\right] \times 10^7 \exp(-273.8p/E_e) & 54 < E_e/p \leq 120 \\ 54.08 \times 10^6 (E_e/p)^{1/2} \exp(-359p/E_e) & 120 < E_e/p \leq 3000 \end{cases} , (29)$$

Considering the collisions of the electron and neutral molecule in
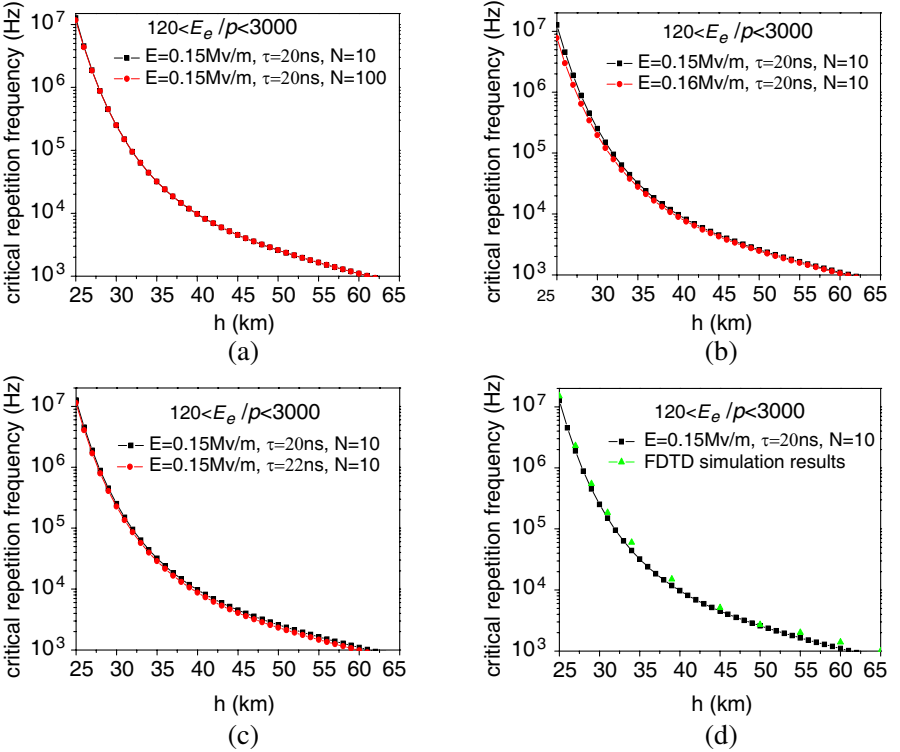
Figure 5. The relation between the critical repetition frequency and the altitude in high-altitude atmosphere for a UWB case. (a) different pulse number N; (b) different electrical field intensity E_e; (c) different single-pulse width τ; (d) the comparison between the FDTD simulation and the semi-analytical calculation.

the atmosphere, we have the electron momentum equation as [20].

$$\partial u/\partial t + v_c u = qE/m, \tag{30}$$

By the Laplace transform, we can write the solution of (30) with the initial electron velocity being zero as

$$u(t) = q/m e^{-v_c t} * E(t), \tag{31}$$

where "∗" indicates the convolution operation.

Combining Equations (26), (27) and (31), we can rewrite the effective field E_e as

$$E_e = \sqrt{\frac{1}{2} \left\langle \left[e^{-\tau v_c} * E(\tau) \right]^2 \right\rangle v_c}. \tag{32}$$
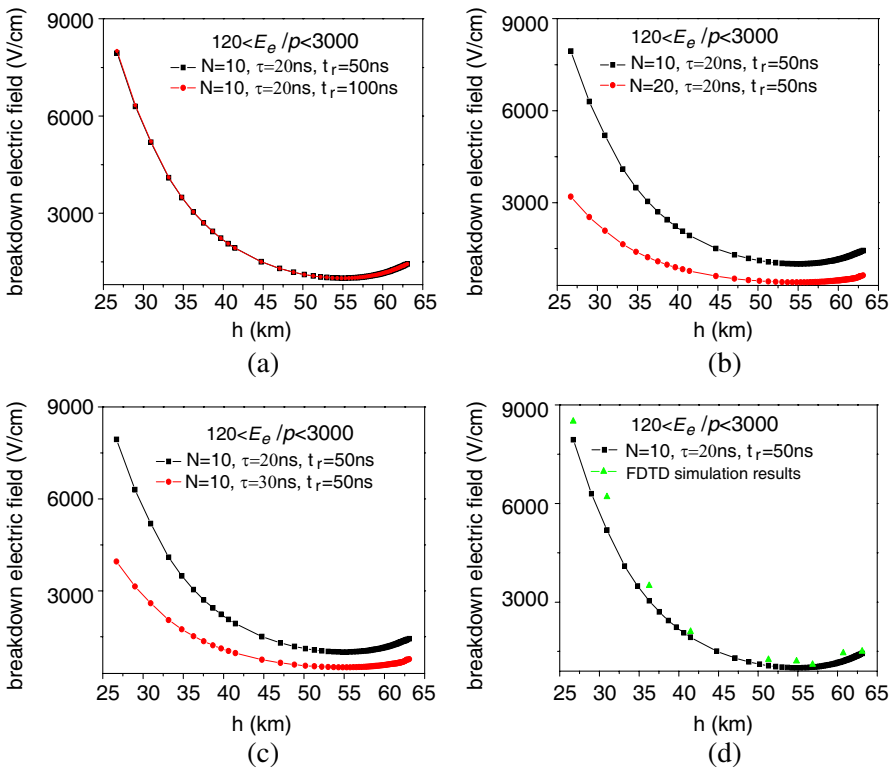
Figure 6. The relation between the breakdown threshold and the altitude in high-altitude atmosphere for a UWB case. (a) different relaxation time t_r; (b) different pulse number N; (c) different single-pulse width τ; (d) the comparison between the FDTD simulation and the semi-analytical calculation.

Plugging Equations (29) and (32) into (10), finally we can obtain the critical repetition frequency f_c of the UWB pulses. Combining Equations (11), (28) and (32), we can obtain the air breakdown threshed.

Now, we take a Gaussian repetition frequency pulse as an UWB example. The Gaussian repetition frequency is composed of a series of single Gaussian pulses with same parameters, which can be written as

$$E(t) = E_0 \cdot \exp\left[-4\pi \left(t - t_0\right)^2 / \tau^2\right], \tag{33}$$

where $t_0 = \tau/2$ and E_0 is the field amplitude.

Figures 5 and 6 show the critical repetition frequency and the air breakdown threshold for the Gaussian repetition frequency pulse with different parameteres in the case of $120 < E_e/p \leq 3000$. The comparison of the simulation results between the semi-analytical model and FDTD are also given in Figs. 5(d) and Fig. 6(d), from which we can see that these two solutions agree with each other very well.

4. CONCLUSION

In this paper, we present a semi-analytical model for the propagation of the repetition frequency HPM pulses in the atmosphere. Basing on the analysis of the minimum relaxation time between the pulses, we derived the critical repetition frequency and the air breakdown threshold for the repetition frequency HPM pulses. The accuracy of these predictions of the semi-analytical model has been demonstrated by the Numerical simulations of the FDTD method. Since the semi-analytical model is highly efficient and very accurate, it is very useful to get quick estimations on the critical repetition frequency and the air breakdown threshold for the propagation of the HPM pulses in the atmosphere.

REFERENCES

1. Pai, S. T. and Q. Zhang, *Introduction to High Power Pulse Technology*, World Scientific, Singapore, 1995.

2. Martin, T. H., M. Williams, and M. Kristiansen, *J. C. Martin on Pulsed Power*, Plenum Press, New York, 1996.

3. Kitsanov, S. A., A. I. Klimov, S. D. Korovin, I. K. Kurkan, I. V. Pegel, and S. D. Polevin, "A vircator with electron beam premodulation based on high-current repetitively pulse accelerator," *IEEE Transactions on Plasma Science*, Vol. 30, No. 1, 278–285, 2002.

4. Soliman, M. S., T. Morimoto, and Z. I. Kawasaki, "Three-dimensional localization system for impulsive noise sources using ultra-wideband digital interferometer technique," *Journal of Elelctromagnetics Wave and Applications*, Vol. 20, No. 4, 515–530, 2006.

5. Golestani-Rad, L. and J. Rashed-Mohassel, "Rigorous analysis of EM-wave penetration into a typical room using FDTD method: The transfer function concept," *Journal of Elelctromagnetics Wave and Applications*, Vol. 20, No. 7, 913–926, 2006.

6. Hwang, S. M., J. I. Hong, and C. S. Huh, "Characterization of the susceptibility of integrated circuits with induction caused by high power microwaves," *Progress In Electromagnetics Research*, Vol. 81, 61–72, 2008.

7. Mesyats, G. A., V. G. Shpak, M. I. Yalandin, and S. A. Shunailov, "Compact high-current repetitive pulse accelerators," *Pulse Power Conf.*, 73–77, San Diego, USA, Jun. 1991.

8. Cao, J. K., D. F. Zhou, Z. X. Niu, Y. Shao, W. Zou, and Z. W. Xing, "Air breakdown by repetition-rate high power microwave pulse," *High Power Laser and Particle Beams*, Vol. 18, No. 1, 115–118, 2006, (in Chinese).

9. Hu, T., D. F. Zhou, Q. R. Li, and Z. X. Niu, "Effect of electronic relaxation process on air breakdown caused by repetition frequency HPM," *High Power Laser And Particle Beams*, Vol. 21, No. 4, 545–549, 2009, (in Chinese).

10. Kuo, S. P., Y. S. Zhang, and K. Paul, "Propagation of high power microwave pulses in air breakdown environment," *Phys. Fluids*, Vol. 133, No. 10, 2906–2912, 1991.

11. Duan, Y. Y. and Y. S. Chen, "Air breakdown of high power microwave pulse and its effect on transmitted energy," *Journal of Microwaves*, Vol. 16, No. 3, 260–264, 2000 (in Chinese).

12. Woo, W. and J. S. DeGroot, "Micowave absorption and plasma

heating due to microwave breakdown in the atmosphere," *Phys. Fluids*, Vol. 27, No. 2, 475–487, 1984.

13. Yee, J. H., D. J. Mayhall, G. E. Sieger, and R. A. Alvarez, "Propagation of intense microwave pulses in air and in a waveguide," *IEEE Trans. on Antennas and Propagation*, Vol. 39, No. 9, 1421–1426, 1991.

14. MacDonald, A. D., *Microwave Breakdown in Gases*, Wiley, New York, 1966.

15. Niu, Z. X., D. J. Yu, J. H. Yang, D. F. Zhou, and D. T. Hou, "Non-linear attenuation of high power microwave propagation in atmosphere," *Journal of Information Engineering University*, Vol. 5, No. 2, 115–117, 2004 (in Chinese).

16. Anderson, D. and M. Lisak, "Breakdown in air-filled microwave waveguides during pulsed operation," *J. Appl. Phys.*, Vol. 56, No. 5, 1414–1419, 1984.

17. Hou, D. T., D. F. Zhou, Z. X. Niu, and Z. Q. Yu, "Effect on air refraction index by effective electric-field intensity in high power microwave propagation," *High Power Laser And Particle Beams*, Vol. 16, No. 9, 1183–1185, 2004 (in Chinese).

18. Löfgren, M., D. Anderson, M. Lisak, and L. Lundgren, "Breakdown-induced distortion of high-power microwave pubes in air," *Phys. Fluids*, Vol. B3, No. 12, 3528–3531, 1991.

19. Tang, T., C. Liao, and D. Yang, "Feasibility study of solving high-power microwave propagation in the atmosphere using FDTD method," *Chinese Journal of Radio Science*, Vol. 25, No. 1, 122–126, 2010.

20. Scholfield, D. W., J. M. Gahl, and N. Shimomura, "Effective electric field for an arbitrary electromagnetic pulse," *IEEE Trans. on Plasma Science*, Vol. 27, No. 2, 628–632, 1999.

21. Ali, A. W., "Nanosecond air breakdown parameters for electron and microwave beam propagation," *Laser and Particle Beams*, Vol. 6, 105–117, 1988.